LETTERS

Petrology and thermal structure of the Hawaiian plume from Mauna Kea volcano

Claude Herzberg[1]

There is uncertainty about whether the abundant tholeiitic lavas on Hawaii are the product of melt from peridotite or pyroxenite/eclogite rocks[1,2]. Using a parameterization of melting experiments on peridotite[3] with glass analyses from the Hawaii Scientific Deep Project 2 on Mauna Kea volcano[1], I show here that a small population of the core samples had fractionated from a peridotite-source primary magma. Most lavas, however, differentiated from magmas that were too deficient in CaO and enriched in NiO (ref. 2) to have formed from a peridotite source. For these, experiments indicate that they were produced by the melting of garnet pyroxenite, a lithology that had formed in a second stage by reaction of peridotite with partial melts of subducted oceanic crust[2]. Samples in the Hawaiian core are therefore consistent with previous suggestions that pyroxenite occurs in a host peridotite, and both contribute to melt production[2,4]. Primary magma compositions vary down the drill core, and these reveal evidence for temperature variations within the underlying mantle plume. Mauna Kea magmatism is represented in other Hawaiian volcanoes, and provides a key for a general understanding of melt production in lithologically heterogeneous mantle.

Variations in MgO and SiO_2 for glasses[1] and whole rocks[5] from Mauna Kea obtained from the Hawaii Scientific Drilling Project 2 (HSDP2) are summarized in Fig. 1a. All lavas are tholeiitic, but there are three main populations of data: a low- and a high-silica population, both of which are uniformly low in CaO, and a small population with low SiO_2 and high CaO and K_2O. A fourth group at 2,233 metres below sea level (m.b.s.l.) in the drill core is similar to the low-SiO_2 type except that it is higher in alkalis[1]. Within the HSDP2 core, the low- and high-SiO_2 lavas are the most abundant, and they are observed in both whole rocks and glasses. The high-CaO types are more rarely found as glasses at 1800 mbsl in the drill core, and a few surface whole rock samples[6,7].

The less-common lavas with the highest CaO contents have the properties of forming from a mantle peridotite source. A primary magma is a partial melt of a mantle source, and several compositions are shown in Fig. 1b and given in Table 1. These have been calculated using a petrological method discussed in Herzberg and O'Hara[8] and summarized in the footnote to Table 1. Peridotite-source primary magmas for Mauna Kea are very similar to those for other picrites and komatiites. All have about 10% CaO, 17–19% MgO, and 46–47% SiO_2, but Mauna Kea differs in having much larger abundances of TiO_2, K_2O, and all other incompatible elements. The 10% CaO is consistent with the new parameterization of CaO shown in Fig. 1b (Supplementary Figs 1–3). That is, the CaO contents of accumulated fractional melts of mantle peridotite do not change much over a wide range of initial and final melting pressures within the garnet lherzolite stability field. Although this result was modelled from experiments on a fertile peridotite[3], there is some indication that it applies also to more depleted compositions. Gorgona komatiites melted from a source with long-term light rare-earth elements depletion[9] (that is, $\varepsilon_{Nd} = +6$–10), indicating that the peridotite source might also be depleted in CaO and Al_2O_3; however, primary magmas consistently display CaO contents of about 10% (Table 1).

The CaO contents of the commoner low- and high-SiO_2 parental magmas were estimated to be about 8.6 and 8.9% CaO, respectively[1]. Parental magmas are the most magnesian liquids that can be inferred from erupted lavas, and they are modified to some extent by fractional crystallization and/or mixing and crystal accumulation. Their compositions have been inferred by calculating liquid compositions that would crystallize $Fo_{90.5}$ olivine, the maximum observed[1]. These parental magmas have significantly less than 10% CaO in peridotite partial melts (Fig. 1b). Therefore, a normal peridotite source is inconsistent with these low-CaO contents (see Supplementary Information), a conclusion that can also be extended to most shield-building tholeiitic lavas from Hawaii. This result is not compromised by augite crystallization, which lowers CaO only when the parental magma evolves by olivine fractionation to about 7.5% MgO. A pyroxenite source was an alternative favoured by Sobolev *et al.*[2] because the Ni contents of most Hawaiian parental magmas and their crystallizing olivines are higher than expected for a peridotite source.

A pyroxenite model for the production of the voluminous low- and high-SiO_2 lavas is shown in Fig. 2. These are projections of lava compositions and phase diagrams that have been constructed from melting experiments (Supplementary Information). Liquids (L) of interest form an array of compositions (similar to Hawaiian primary magmas) that project along a line called a cotectic because they co-crystallize orthopyroxene, clinopyroxene and garnet [L+opx+cpx+gt]. The pyroxene–garnet plane is a thermal divide that separates cotectic liquids on each side from being derived from each other either by partial melting or crystallization[10–12]. To visualize the thermal divide, these liquid compositions are projected to and from diopside into the plane olivine–quartz–CATS (calcium Tschermak's pyroxene), a Kogiso diagram[12] (Fig. 2a). Pyroxene and garnet compositions project along the line opx–CATS. The cotectic [L+opx+cpx+gt] consists of two segments separated by the thermal divide. The first segment is defined by liquids that become increasingly olivine-rich as temperature decreases, in blue in Fig. 2; the compositions of these liquids are well-known at 3 GPa, but only moderately constrained at 4 GPa (Supplementary Information). The second segment is defined by liquids that become increasingly SiO_2-rich as temperature decreases, in red in Fig. 2; the projected locations in Fig. 2 have been interpolated from experiments on natural MORB compositions crystallizing [L+cpx+gt+quartz or coesite][13,14] (Supplementary Information). There is some confidence about this interpolation from theoretical considerations (Supplementary Information), but calibration by additional experimental work is needed.

[1]Department of Geological Sciences Rutgers University Piscataway, New Jersey 08854, USA.

Table 1 | Estimated compositions of peridotite-source primary magmas for Mauna Kea and other occurrences

	Mauna Kea samples				Gorgona	Baffin Island	West Greenland
	SR0684-8.95 (ref. 1)	SR0684-9.00 (ref. 1)	KI-8 (ref. 6)	C-209 (ref. 7)			
SiO_2	46.3	46.4	46.47	45.84	46.1	46.5	46.9
TiO_2	2.01	2.11	1.78	1.83	0.56	0.99	1.29
Al_2O_3	9.93	9.93	8.6	9.9	11.7	12.1	11.6
Cr_2O_3	-	-	0.26	-	0.16	0.09	0.05
Fe_2O_3	0.93	0.90	1.24	1.23	1.18	0.99	1.82
FeO	10.4	10.1	10.3	10.32	10.1	9.7	9.4
MnO	0.18	-	0.16	0.19	0.18	0.17	0.21
MgO	17.8	18.1	19.0	18.27	18.8	17.9	17.1
CaO	10.0	10.0	10.1	10.12	10.0	10.1	9.9
Na_2O	1.72	1.69	1.73	1.53	1.04	1.30	1.56
K_2O	0.56	0.52	0.12	0.42	0.03	0.04	0.09
NiO	-	-	0.079	0.084	0.112	0.110	0.081
P_2O_5	0.234	0.202	0.186	0.284	-	-	-
k_d	0.298	0.298	0.299	0.296	0.300	0.301	0.303
Olivine Mg#	91.1	91.4	91.6	91.4	91.7	91.6	91.5
T (oC)	1,405	1,411	1,428	1,414	1,425	1,407	1,391

Primary magmas are estimated with a hybrid forward and inverse model discussed in ref. 8. The forward model component identifies all potential primary magma compositions as functions of melt fraction for an assumed peridotite source and melting mechanism, based on a parameterization of experimental data. These are displayed in projections and FeO–MgO plots, and accumulated fractional melting is the mechanism assumed here. The inverse component selects a derivative liquid in an erupted lava suite into which olivine is incrementally added; this provides an array of possible primary magma composition. The potential primary magmas in both forward and inverse models are compared, and common melt fractions in both projection and FeO–MgO plots are used to seek a unique primary magma solution. Primary magma solutions are usually the same for both fertile and depleted peridotite sources with FeO ≅ 8 wt%. Olivine is added to the four Mauna Kea samples shown. The Fe–Mg exchange coefficient k_d for olivine–L and Mg# for olivine are calculated using the method of Toplis[29] and FeO/ΣFe = 0.90. T (°C) is the olivine liquidus temperature calculated at 1 atmosphere using the method of Beattie[30]. Primary magmas for komatiites from Gorgona komatiites, and picrites from Baffin Island and West Greenland are given for comparison[8].

HSDP2 glasses with >7.5% MgO exhibit no signs of augite or plagioclase fractionation. To these samples olivine was added until the liquid reached the cotectic [L+opx+cpx+gt], yielding primary pyroxenite-source magmas. Many of these are very similar to parental magmas that have been independently estimated with $Fo_{90.5}$ olivine as a constraint[1], which suggests no change in primary magma composition during transit from the mantle to the crust. Representative compositions are given in Table 2. Figure 2 shows that high-SiO_2 parental and primary magmas project to the SiO_2-rich side of the thermal divide. In contrast, low-SiO_2 parental and primary magmas project to the olivine-rich side of the divide. There is a clear separation of these two populations of data, indicating that they are partial melts of garnet pyroxenite formed on the cotectic [L+opx+cpx+gt]. Whole-rock data are similar, but they are less separated than the glasses. This work supports models of pyroxenite within a peridotite matrix for Hawaii, and melt production from both sources[2,4] (Figs 1b, 2).

The thermal divide predicts primary magma compositions on each side will become increasingly similar with increasing temperature and, indeed, this is seen in Fig. 3a for Na_2O, P_2O_5 and SiO_2 abundances from the glass data. This agreement between theory and observation is a positive test of the importance of pyroxenite melting along the cotectic [L+opx+cpx+gt]. Some of the scatter in the trends might be a reflection of original pyroxenite source heterogeneity. In contrast, whole rocks exhibit no such behaviour (Fig. 3b) for Na_2O or any other incompatible element, although both SiO_2 populations generally project on each side of the thermal divide. Some of the whole-rock variability arises by addition and subtraction of augite and plagioclase[5], which has been filtered out (Supplementary Information) to obtain as much of the partial melting signature

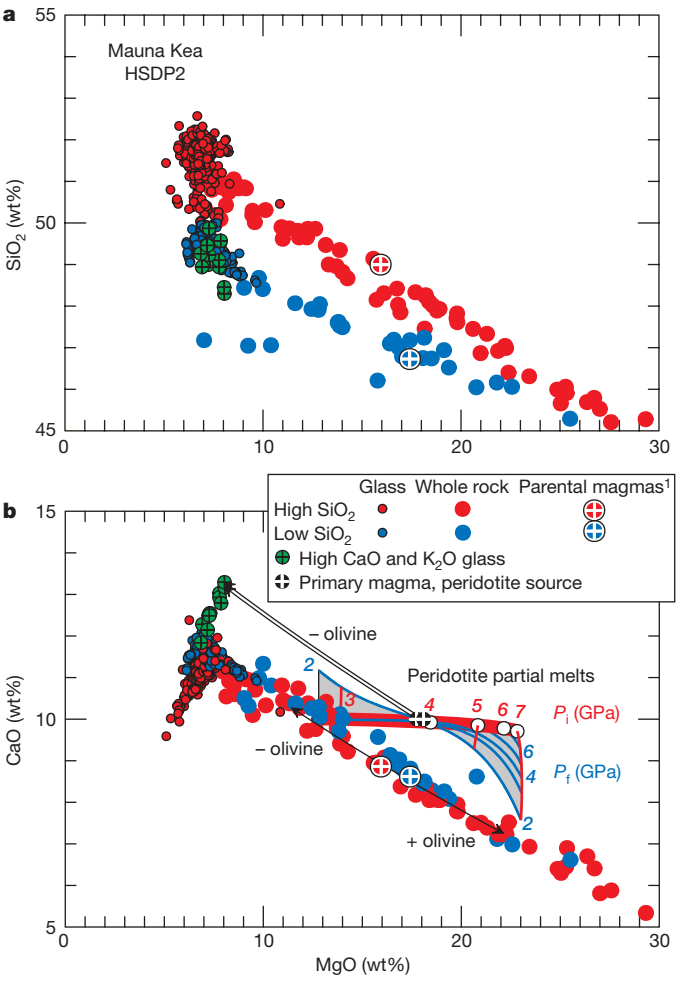

Figure 1 | Geochemical variations in Mauna Kea lavas from the Hawaii Scientific Drilling Project 2 (refs 1, 5) compared with estimated compositions of parental and primary magmas. For clarity, only whole-rock samples for which isotopic data also exist are shown. **a,** Variations in MgO and SiO_2 for glass and whole-rock samples. **b**, Variations in MgO and CaO glass and whole-rock samples compared with primary magmas of fertile mantle peridotite, formed by accumulated fractional melting (see Supplementary Information). Several glasses with high CaO and K_2O could have formed by olivine fractionation from the peridotite-source primary magmas. Parental magmas in equilibrium with $Fo_{90.5}$ olivine[1] for commoner low- and high-SiO_2 lavas have CaO contents that are too low to qualify as partial melts and primary magmas of normal mantle peridotite. Black arrows in **b** display the effects of olivine addition (right pointing) and subtraction (left pointing) for the primary and parental magmas. Accumulated fractional melt compositions are shaded in grey, with red lines defining initial melting pressures P_i and blue lines defining final melting pressures P_f. Solidus melts are shown as white circles connected with a thick red line. Examples of how to read this diagram are given as a tutorial in the Supplementary Fig. 3 legend.

Table 2 | Estimated compositions of parental magmas and pyroxenite-source primary magmas for Mauna Kea

Type sample number	Low Si (ref. 1)	Low Si (SR0756-11.70)	Low Si (SR0823-17.50)	High Si (ref. 1)	High Si (SR0711-15.50)	High Si (SR0962-4.10)
SiO_2	46.72	47.63	46.6	48.99	48.60	49.45
TiO_2	1.98	1.85	0.92	1.91	2.04	1.84
Al_2O_3	10.52	10.54	10.38	10.56	9.94	10.49
Cr_2O_3	0	0	0	0	0	0
Fe_2O_3	0	0.926	0.983	0	0.873	0.856
FeO	11.76	10.692	10.98	10.79	10.048	9.724
MnO	0.17	0	0	0.17	0	0
MgO	17.42	17.44	18.44	15.95	17.25	16.56
CaO	8.62	8.79	8.43	8.86	9.12	8.87
Na_2O	1.81	1.69	1.83	1.74	1.61	1.78
K_2O	0.29	0.28	0.28	0.3	0.29	0.28
NiO	0	0	0	0	0	0
P_2O_5	0.16	0.143	0.15	0.16	0.227	0.159
k_d	0.320	0.306	0.301	0.320	0.310	0.313
Olivine Mg#	90.5	90.5	90.9	90.5	90.8	90.6
T (oC)	1,398	1,398	1,418	1,367	1,394	1,380

Some compositions were estimated by Stolper *et al.*[1]. All other compositions have been estimated by addition of olivine into the sample numbers given, and the calculation was stopped when the composition reached the cotectic [L+opx+cpx+gt]. FeO/ΣFe is assumed to be 0.90 in samples before olivine addition. The Fe–Mg exchange coefficient k_d for olivine–L and Mg# for olivine are calculated using the method of Toplis[29] at 1 atmosphere. T (°C) is the olivine liquidus temperature calculated at 1 atmosphere using the method of Beattie[30].

as possible. Nevertheless, whole rocks always exhibit considerable scatter, unlike glasses. These observations indicate that Mauna Kea volcanic glasses may be faithfully recording primary pyroxenite magmas preserved at the micrometre scale. In contrast, whole rocks record considerable averaging of these magmas and do not reveal details of melting at the resolution of glasses. Similar conclusions have been made when comparing analyses of olivine-hosted melt inclusions and whole rocks[4,15].

Figure 4 depicts the pyroxenite-source primary magma compositions that gave rise to the lavas as sampled in the drill core. The position of the primary magmas with respect to the thermal divide is particularly revealing in SiO_2, which imposes a rough symmetry for low- and high-SiO_2 magmas. The hottest primary magmas are identified at about 2,100 m.b.s.l. in the drill core where the low- and high-SiO_2 primary magmas are most similar in SiO_2. A drop in magmatic temperature can be inferred above and below 2,100 m.b.s.l., where SiO_2 decreases and MgO increases for the low-SiO_2 primary pyroxenite magmas. This behaviour for MgO might be counter-intuitive, but liquids change in this way when temperatures decrease for the cotectic [L+opx+cpx+gt] on the olivine-rich side of the divide. For reasons that are not clear, the glasses have somewhat lower Al_2O_3 than do the whole rocks, and this yields primary magmas with higher MgO contents. Small variations in Al_2O_3 are responsible for the variable and noisy MgO signal, but SiO_2 is not as strongly affected.

I interpret the rough stratigraphic symmetry seen in Fig. 4 to mean a constant source temperature at any specific level in the core, and temperature-induced changes with time. Temporal variations in the raw glass compositions were also discussed by Stolper *et al.*[1], but they occur at different core depths, indicating a separate part played by magma chambers or melt transport[1]. The temperature variations

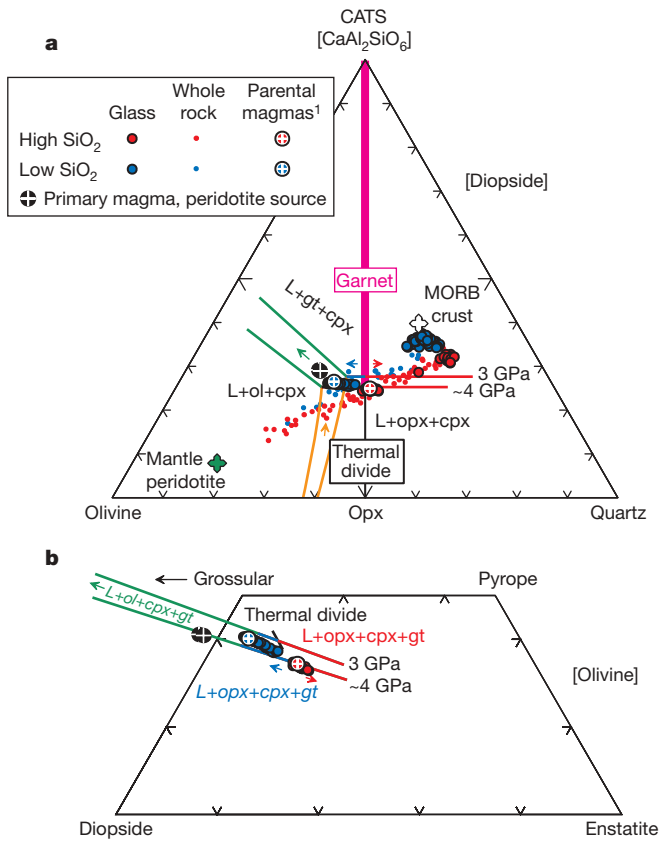

Figure 2 | Projections of HSDP2 whole rocks and glasses compared with cotectics at 3 and 4 GPa, which are arrays of liquid compositions that co-crystallize various crystalline phases. Of special interest here is the cotectic that defines liquid compositions that co-crystallize orthopyroxene, clinopyroxene and garnet [L+opx+cpx+gt], in blue and red for segments on the olivine-rich and SiO_2-rich sides of the thermal divide, respectively. Other cotectics are [L+olivine+opx±cpx], in brown, and [L+olivine+cpx+gt], in green. The projected cotectics are discussed in the Supplementary Information. Glasses have been filtered out to include only those samples that have experienced olivine fractionation (that is, >7.5% MgO). Mid-ocean-ridge basalt (MORB) crust is the experimental composition used by ref. 13. Peridotite composition is from ref. 14. **a**, A mole% projection from or towards diopside into the plane olivine–quartz–CATS. The pyroxene–garnet plane is represented by the line CATS–opx, and it is a thermal divide, as shown by opposing arrows next to the cotectic [L+opx+cpx+gt]. Shown are individual glass analyses from ref. 1 that plot furthest from olivine, and the same glass analyses into which olivine was added until the desired composition reached the cotectic [L+opx+cpx+gt]; these are primary pyroxenite magma compositions. **b**, A mole% projection from or towards olivine into part of the pyroxene–garnet plane. High-SiO_2 glasses are coincident with the cotectic [L+opx+cpx+gt] on the silica-rich side of the thermal divide in Fig. 2a, shown in red. Low-SiO_2 glasses are coincident with the cotectic [L+opx+cpx+gt] on the olivine-rich side of the thermal divide in Fig. 2a, shown in blue. The parental magmas of ref. 1 are very similar to primary magmas of pyroxenite. For whole rocks, the low- and high-SiO_2 populations generally project on each side of the thermal divide and, although this is not shown for purposes of clarity, there is considerable overlap (Supplementary Information). A three-dimensional geochemical representation is obtained by a simultaneous visualization of panels **a** and **b**. Diopside and enstatite are pyroxenes: $Ca(Mg,Fe)Si_2O_6$ and $(Mg,Fe)_2Si_2O_6$. Grossular and pyrope are garnets: $Ca_3Al_2Si_3O_{12}$ and $(Mg,Fe)_3Al_2Si_3O_{12}$.

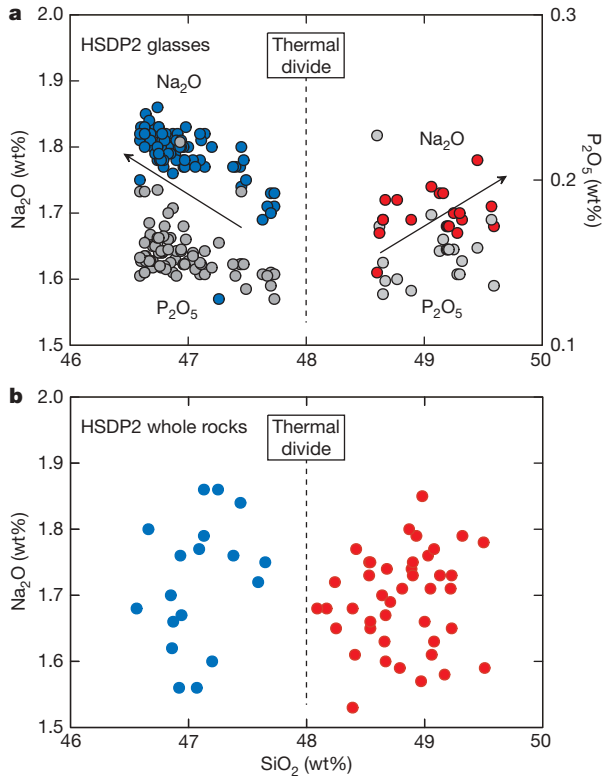

Figure 3 | Na_2O and P_2O_5 proxies for temperature along the cotectic [L+opx+cpx+gt]. Maximum temperatures occur at the thermal divide for primary magmas near the pyroxene–garnet plane, where liquids contain ~48% SiO_2. Arrows point in the direction of decreasing temperature. For constant pyroxenite source composition, liquids near this plane are predicted to have minimum contents of Na_2O and P_2O_5. **a**, Primary pyroxenite magma compositions determined from glass analyses. Glasses identified by ref. 1 at 2,233 m.b.s.l. are similar to low-SiO_2 types, but they are highest in Na_2O and MgO, and plot at the lowest temperatures in this group. **b**, Primary pyroxenite magma compositions determined from whole-rock analyses filtered to exclude samples for which there has been minor plagioclase and augite addition and subtraction (see Supplementary Information).

displayed by the low-SiO_2 primary pyroxenite magmas are expected to be 30–50 °C, based on the following temperatures at 3 GPa: 1,560–1,580 °C near the thermal divide[16,17], and 1,515–1,540 °C at the olivine termination of the cotectic [L+ol+opx+cpx+gt][3,8]. Peridotite-source melts appear briefly at about 1,800 m.b.s.l., and these will have a 3 GPa liquidus temperature of about 1,550 °C (ref. 8) and a potential temperature that is also 1,550 °C; initial and final melting pressures are about 4.0 and 3.0 GPa, respectively. Pyroxenite source temperature variations translate to potential temperatures of ~1,500–1,550 °C. This is evidence for magmatic sampling of different temperature domains within the plume, the axis being the hottest.

Temperatures are 1,470–1,500 °C at the 3 GPa anhydrous peridotite solidus[18,19] and 1,560–1,580 °C near the thermal divide[16,17]. It is therefore possible for pyroxenite melts with compositions along the cotectic [L+opx+cpx+gt] and near the thermal divide to be hotter than peridotite melts even though they are lower in MgO. The common petrological practice of using MgO in a primary magma to infer volcanic and source temperature conditions should be made judiciously, and is only secure when the source is olivine-bearing.

The Hawaiian tholeiites cannot be single-stage partial melts of an original basaltic crustal protolith of bimineralic eclogite or quartz/coesite eclogite[13,14] at 3.0–3.5 GPa because they are too high in NiO and MgO, and too low[2,13] in SiO_2 and Al_2O_3 (Fig. 2). Sobolev *et al.*[2] proposed that the pyroxenite source forms in a second stage by melt-rock reaction. At 3 GPa, quartz eclogite begins to melt at about 1,315 °C[13] and the SiO_2-rich melts can react with the peridotite host to produce[14,20] opx+cpx+gt (Supplementary Information). Orthopyroxene may be heavily concentrated in bands, as indicated by experiment[14,20] and metasomatic theory[2,21], but primary magmas will form at contacts with cpx and gt where the temperatures are at a minimum on the cotectic [L+opx+cpx+gt]. Large melt fractions of pyroxenite may be temporarily entombed by these orthopyroxene-rich reaction zones[22], but leaks might refertilize the surrounding peridotite.

The phase diagram in Fig. 2 provides a key for a general understanding of melt production in lithologically heterogeneous mantle. Unlike pyroxenite melting below other oceanic islands on Earth, pyroxenite melts with compositions on the SiO_2-rich side of the thermal divide are unique to the shield-building lavas of Hawaii. And, unlike Mauna Kea, there is no evidence for the involvement of peridotite-source melts below Mauna Loa and Kilauea. For all shield-building lavas on Hawaii, the phase diagram requires a substantial role for SiO_2-rich basaltic oceanic crust (Fig. 2a). This is

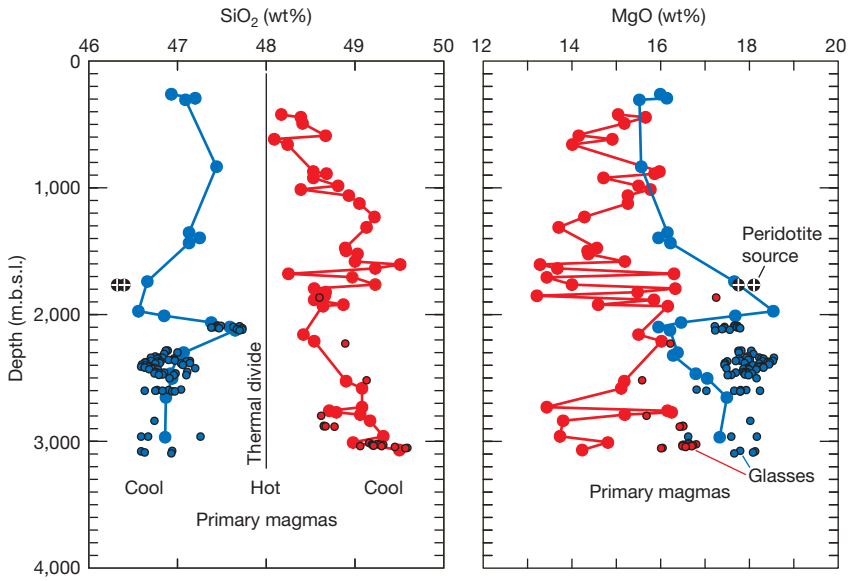

Figure 4 | Variations in SiO_2 and MgO contents of pyroxenite primary magma compositions for glasses and whole rocks with depth in the HSDP2 drill core. Whole-rock analyses have been filtered to exclude samples for which there has been minor plagioclase and augite addition and subtraction; these are connected by the blue (SiO_2-poor) and red (SiO_2-rich) lines. Glasses have been filtered to include only those samples that have experienced olivine fractionation (that is, >7.5% MgO). Core locations are shown in metres below sea level (m.b.s.l.). SiO_2 contents of pyroxenite primary magmas are good proxies for temperatures of their source, with maximum temperatures realized for magmas with ~48% SiO_2 produced nearest the thermal divide.

supporting evidence for previous suggestions that recycled crust is organized in large bodies[23,24], reconstituted as pyroxenite[2]. The implication is that oceanic crust has been subducted, stirred, stretched and returned in a plume with its fine structure roughly preserved as geochemical heterogeneities in Hawaiian volcanoes[15,25–28]. This improbable idea seems quite reasonable from a petrological point of view.

Received 2 March; accepted 13 September 2006.

1. Stolper, E., Sherman, S., Garcia, M., Baker, M. & Seaman, C. Glass in the submarine section of the HSDP2 drill core, Hilo, Hawaii. *Geochem. Geophys. Geosyst.* **5,** doi:10.1029/2003GC000553 (2004).
2. Sobolev, A. V., Hofmann, A. W., Sobolev, S. V. & Nikogosian, I. K. An olivine-free mantle source of Hawaiian shield basalts. *Nature* **434,** 590–597 (2005).
3. Walter, M. J. Melting of garnet peridotite and the origin of komatiite and depleted lithosphere. *J. Petrol.* **39,** 29–60 (1998).
4. Ren, Z-Y., Ingle, S., Takahashi, E., Hirano, N. & Hirata, T. The chemical structure of the Hawaiian plume. *Nature* **436,** 837–840 (2005).
5. Rhodes, J. M. & Vollinger, M. J. Composition of basaltic lavas sampled by phase-2 of the Hawaii Scientific Drilling Project: geochemical stratigraphy and magma types. *Geochem. Geophys. Geosyst.* **5,** doi:10.1029/2002GC000434 (2004).
6. Frey, F. A. *et al.* The evolution of Mauna Kea volcano, Hawaii: petrogenesis of tholeiitic and alkalic basalts. *J. Geophys. Res. B* **96,** 14347–14375 (1991).
7. Sobolev, A. V. & Nikogosian, I. K. Petrology of long-lived mantle plume magmatism: Hawaii, Pacific, and Reunion islands, Indian Ocean. *Petrology* **2,** 111–144 (1994).
8. Herzberg, C. & O'Hara, M. J. Plume-associated ultramafic magmas of Phanerozoic age. *J. Petrol.* **43,** 1857–1883 (2002).
9. Arndt, N. T., Kerr, A. C. & Tarney, J. Dynamic melting in plume heads: the formation of Gorgona komatiites and basalts. *Earth Planet. Sci. Lett.* **146,** 289–301 (1997).
10. O'Hara, M. J. & Yoder, H. S. Jr. Formation and fractionation of basic magmas at high pressures. *Scott. J. Geol.* **3,** 67–117 (1967).
11. Milholland, C. S. & Presnall, D. C. Liquidus phase relations in the CaO-MgO-Al_2O_3-SiO_2 system at 3.0 GPa: The aluminous pyroxene thermal divide and high pressure fractionation of picritic and komatiitic magmas. *J. Petrol.* **39,** 3–27 (1998).
12. Kogiso, T., Hirschmann, M. M. & Pertermann, M. High-pressure partial melting of mafic lithologies in the mantle. *J. Petrol.* **45,** 2407–2422 (2004).
13. Pertermann, M. & Hirschmann, M. M. Anhydrous partial melting experiments on MORB-like eclogite: phase relations, phase compositions and mineral-melt partitioning of major elements at 2–3 GPa. *J. Petrol.* **44,** 2173–2201 (2003).
14. Yaxley, G. M. & Green, D. H. Reactions between eclogite and peridotite: mantle refertilisation by subduction of oceanic crust. *Schweiz. Mineral. Petrogr. Mitt.* **78,** 243–255 (1998).
15. Sobolev, A. V., Hofmann, A. W. & Nikogosian, I. K. Recycled oceanic crust observed in 'ghost plagioclase' within the source of Mauna Loa lavas. *Nature* **404,** 986–989 (2000).
16. Ito, K. & Kennedy, G. C. Melting and phase relations in the plane tholeiite-lherzolite-nepheline basanite to 40 kilobars and geological implications. *Contrib. Mineral. Petrol.* **19,** 177–211 (1968).
17. Maaloe, S. The PT-phase relations of an MgO-rich Hawaiian tholeiite: the compositions of primary Hawaiian tholeiites. *Contrib. Mineral. Petrol.* **148,** 236–246 (2004).
18. Hirschmann, M. M. Mantle solidus: experimental constraints and the effects of peridotite composition. *Geochem. Geophys. Geosyst.* **1,** doi:10.1029/2000GC000070 (2000).
19. Herzberg, C., Ratteron, P. & Zhang, J. New experimental observations on the anhydrous solidus for peridotite KLB-1. *Geochem. Geophys. Geosyst.* **1,** doi:10.1029/2000GC000089 (2000).
20. Takahashi, E. & Nakajima, K. in *Hawaiian Volcanoes: Deep Underwater Perspectives* (eds Takahashi, E., Lipman, P. W., Garcian, M. O., Naka, J. & Aramaki, S.) Vol. 128, 403–418 (Geophys. Monogr. Ser., AGU, Washington DC, 2002).
21. Korzhinskii, D. S. *Theory of Metasomatic Zoning* (Clarendon, Oxford, 1970).
22. Kogiso, T., Hirschmann, M. M. & Reiners, P. W. Length scales of mantle heterogeneities and their relationship to ocean island basalt geochemistry. *Geochim. Cosmochim. Acta* **68,** 345–360 (2004).
23. Abouchami, W. *et al.* Lead isotopes reveal bilateral asymmetry and vertical continuity in the Hawaiian mantle plume. *Nature* **434,** 851–856 (2005).
24. Blichert-Toft, J., Weis, D., Maerschalk, C., Agranier, A. & Albarède, F. Hawaiian hot spot dynamics as inferred from the Hf and Pb isotope evolution of Mauna Kea volcano. *Geochem. Geophys. Geosyst.* **4,** doi:10.1029/2002GC000340 (2003).
25. Lassiter, J. C. & Hauri, E. H. Osmium-isotope variations in Hawaiian lavas: evidence for recycled lithosphere in the Hawaiian plume. *Earth Planet. Sci. Lett.* **164,** 483–496 (1998).
26. Blichert-Toft, J., Frey, F. A. & Albarède, F. Hf isotope evidence for pelagic sediments in the source of Hawaiian basalts. *Science* **285,** 879–882 (1999).
27. Huang, S. *et al.* Enriched components in the Hawaiian plume: Evidence from Kahoolawe volcano, Hawaii. *Geochem. Geophys. Geosyst.* **6,** doi:10.1029/2005GC001012 (2005).
28. Hauri, E. Major element variability in the Hawaiian plume. *Nature* **382,** 415–419 (1996).
29. Toplis, M. J. The thermodynamics of iron and magnesium partitioning between olivine and liquid: criteria for assessing and predicting equilibrium in natural and experimental systems. *Contrib. Mineral. Petrol.* **149,** 22–39 (2005).
30. Beattie, P. Olivine-melt and orthopyroxene-melt equilibria. *Contrib. Mineral. Petrol.* **115,** 103–111 (1993).

Supplementary Information is linked to the online version of the paper at www.nature.com/nature.

Acknowledgements I am grateful to A. Sobolev, M. Feigenson, M. Hirschmann, F. Frey and P. Asimow for discussions. I also thank A. Hofmann and A. Sobolev for critical comments.

Author Information Reprints and permissions information is available at www.nature.com/reprints. The authors declare no competing financial interests. Correspondence and requests for materials should be addressed to C.H. (herzberg@rci.rutgers.edu).